AIMS Mathematics, 10(11): 25545–25567.
DOI: 10.3934/math.20251131
Received: 13 September 2025
Revised: 25 October 2025
Accepted: 29 October 2025
Published: 06 November 2025

https://www.aimspress.com/journal/Math

Research article

Stability and bifurcation of a fractional-order phytoplankton-zooplankton model with Holling type-II response

M. B. Almatrafi*

Department of Mathematics, College of Science, Taibah University, Al-Madinah Al-Munawarah, Saudi Arabia

* **Correspondence:** Email: mmutrafi@taibahu.edu.sa.

Abstract: Fractional-order differential equations have recently been utilized in phytoplankton-zooplankton models to represent genetics influences. These influences are frequently seen in aquatic ecosystems but cannot be completely explained by standard integer-order models. The focus of this work was to analyze the dynamics of a fractional-order phytoplankton-zooplankton model that incorporates a Holling type-II functional response. This model was discretized using the Caputo fractional derivative. We carried out an extensive stability analysis to determine the equilibrium states of the system and establish the requirements under which these points are stable or unstable. We used the bifurcation theory to investigate the development of bifurcations when the parameters of the considered model varied, which showed intricate dynamical features including chaos and oscillations. We analyzed Neimark-Sacker and flip bifurcations using a discretization parameter ω. The chaos control was presented. Computational simulations were executed in order to independently confirm the theoretical results and point out the diverse dynamics that the model displays. Our findings provide further clarification on the interactions between phytoplankton and zooplankton species, demonstrating significant environmental implications for marine ecosystems.

Keywords: conformable fractional derivative; phytoplankton-zooplankton model; discretization; stability analysis; bifurcations; chaos control
Mathematics Subject Classification: 34K37, 26A33, 37M15, 70J50, 34K20, 74H55, 35B32, 37G15, 34H10

1. Introduction

Differential equations have a significant role in the formation and evaluation of biological models because they offer a theoretical basis for clarifying the dynamic behavior of biological phenomena throughout time [1]. Several biological phenomena, for instance growth in populations,

the transmission of transmissible illnesses, tumor-immune interactions, enzyme kinetics, and neural activity, can be expressed as systems of ordinary or partial differential equations. These systems measure the rates of variation in vital variables (e.g., population numbers, concentrations, or cell densities) in response to both internal and external influences. Predator-prey scenarios are one of the greatest widely recognized applications of differential equations in biological mathematics as they present an organized strategy to clarify the dynamic interactions between two organisms, one as the predator and the other as the prey. In particular, the physiological communication between the populations of predators and prey in the natural world is widely acknowledged to be a classical and crucial topic of conversation. The phenomenon of predation can occur between animals, plants, insects, and other organisms. In particular, predation occurs between phytoplankton and zooplankton populations [2]. A variety of aquatic food chains are based on phytoplankton which are microscopic algae that are typically observed on the water's surface. The phytoplankton provide the species that live in lakes, rivers, seas, estuaries, and oceans with essential food and oxygen. Plankton are very small organisms that can move on water. They consist of very small animals (called zooplankton) and very small plants (called phytoplankton). Zooplankton, which represent the predator, eat the phytoplankton, which represent the prey. More specifically, zooplankton feed on phytoplankton to survive, while phytoplankton feed on nutrients. A sophisticated mathematical mechanism for understanding the dynamics of marine ecosystems, with a special emphasis on the interactions between phytoplankton and zooplankton populations, is the fractional-order phytoplankton-zooplankton model. The memory and reproductive components of ecological processes are taken into account by this model, which are important for comprehending the stability and long-term behaviors of ecosystems. The fractional-order approach, which includes derivatives of non-integer orders in contrast to traditional integer-order mathematical models, gives a more detailed description of the intricate temporal and spatial dynamics found in biological structures.

Recently published researches have demonstrated a great interest in fractional-order phytoplankton-zooplankton models. For instance, fractional Routh–Hurwitz stability conditions were nicely implemented in [3] to investigate the local stability of the phytoplankton–zooplankton system. The dynamical behavior of this model is numerically analyzed in [3]. Priyadarsini et al. [4] discussed the utilization of the Laplace transform technique, the Adomain decomposition approach, and the differential transform procedure to deal with the numerical solutions of fractional differential equations involving the phytoplankton-toxic phytoplankton-zooplankton equations. Banach fixed point theory was employed in [5] to demonstrate the existence as well as the uniqueness of the solutions to a recently discovered fractional-order delayed zooplankton–phytoplankton structure. Additionally, Pleumpreedaporn et al. [6] investigated the dynamical consequences of various fractional operators in nutrient-phytoplankton-zooplankton models with a variable-order fractional derivative in the Caputo sense. In order to further clarify the dynamics of nutrient-phytoplankton-zooplankton phenomena, Shi et al. [7] took into consideration a fractional-order mathematical model with time delay. They investigated how time delay and fractional order affected the ecological system and obtained the local stability of the equilibrium points. Moreover, in the context of the Caputo fractional derivative, Premakumari et al. [8] provided a mathematical model that incorporates viral infection events and examined the complicated relationships between nutrients, phytoplankton, and zooplankton populations. A novel dynamical system with delay in time for the plankton population was established by Xu et al. [9]. They extracted the requirements for the existence, uniqueness, and boundedness of

the solutions to the recognized plankton population dynamical problem. Further, utilizing the Hopf bifurcation and stability theory of delayed dynamic systems, Xu et al. [9] examined the formation of Hopf bifurcation and stability characteristics in the well-established plankton population dynamical model. The literature review as a whole indicates that fractional-order phytoplankton-zooplankton models are becoming more and more popular, where the scientists investigate various methods of computation, stability, and dynamical responses in these systems.

The use of fractional-order derivatives in biological phenomena plays a significant role in the description of such events. This can be attributed to the fact that the fractional order acts like a closed spectator, which offers us significantly exact and more reliable data about our system. Moreover, in comparison to integer derivatives, fractional derivatives tend to be more general. The vital transitions in the qualitative behavior of biological models as parameters change are commonly referred to as the bifurcation of bio-mathematics models. Understanding sophisticated biological processes like the evolution of populations, relationships between populations, epidemiology, and cellular control requires an understanding of this phenomenon. In particular, bifurcation theory is a promising technique for identifying the fundamental principles behind complex biological phenomena. This theory examines how minor changes in parameters can result in major modifications in the behavior of the system. This article discusses the dynamics of a fractional-order phytoplankton-zooplankton model with Holling type-II response given by

$$\begin{cases} {}_cD^{\gamma}x(t) = Rx(t)(1-x(t)) - \dfrac{\delta x(t)y(t)}{f+x(t)} - Mx(t)^2, \\ {}_cD^{\gamma}y(t) = \dfrac{cx(t)y(t)}{f+x(t)} - \dfrac{dx(t)y(t)}{f+x(t)} - sy(t), \end{cases} \tag{1.1}$$

where ${}_cD^{\gamma}$ is the Caputo fractional derivative of order γ. The function $\frac{\delta x(t)y(t)}{f+x(t)}$ is the rate at which the phytoplankton population is consumed by the zooplankton population. Further, it causes a rise in the development rate of zooplankton and this development rate is represented by the function $\frac{cx(t)y(t)}{f+x(t)}$. The parametric values in model (1.1) are positive and defined in Table 1. The motivation of this work is to improve our comprehension of phytoplankton-zooplankton communications using a more complicated mathematical structure, eventually leading to more effective predictions in the environment. The novelty of this work is to develop novel theoretical criteria for stability and bifurcation analysis in terms of the fractional order and model parameters. Moreover, we verify these results using computational analysis which is richer and more realistic.

The organization of this manuscript is given as follows. Section 2 provides the main concepts used in this article while Section 3 gives the discretization of system (1.1). In Section 4, we introduce the fixed points of system (3.2) and find stability of this system around these points. Sections 5 and 6 analyze the Neimark-Sacker bifurcation and flip bifurcation, respectively. Furthermore, Section 7 gives an extensive study for the chaos control while Section 8 presents some numerical examples to confirm the theoretical outcomes. Finally, Section 9 discusses the main results while Section 10 presents the conclusion of this work.

Table 1. Biological description of parameters.

Parameter of model (1.1)	Biological description
t	Time
$x(t)$	Population densities of phytoplankton at time t
$y(t)$	Population densities of zooplankton at time t
R	Intrinsic growth rates of the phytoplankton population
δ	Maximal phytoplankton uptake rate of zooplankton
f	The constant of fractional catching saturation
$Mx(t)^2$	Represents the infection of the phytoplankton population by an external toxic substance, where $\frac{d^2(Mx(t)^2)}{dt^2} = 2 > 0$
c	The transformation rate of phytoplankton-zooplankton ($c < \delta$)
d	The rate of toxic substances produced by per unit biomass of phytoplankton
s	Death rate of the zooplankton population

2. Essential principles

In this section, we present the fundamental principles needed to carry out the investigation.

Definition 2.1. *The Caputo definition of fractional derivative of order γ for the continuous function $F : (0, \infty) \to \mathrm{R}$ is represented by the following expression [10]:*

$$ {}_cD^{\gamma}F(t) = \frac{1}{\Gamma(1-\gamma)} \int_0^t (t-\tau)^{-\gamma} F(\tau) d\tau, \quad 0 < \gamma \leq 1, \ \ t > 0. \tag{2.1} $$

Lemma 2.2. *[11, 12] Assume that (u^*, v^*) is a fixed point for the planar system (3.2) with multipliers (eigenvalues of the Jacobian matrix) κ_1 and κ_2. Then:*

1. *If $|\kappa_1| < 1$ and $|\kappa_2| < 1$, then the point (u^*, v^*) is a sink point and locally asymptotically stable.*
2. *If $|\kappa_1| > 1$ and $|\kappa_2| > 1$, then the point (u^*, v^*) is a source point and locally unstable.*
3. *If $|\kappa_1| < 1$ and $|\kappa_2| > 1$ (or $|\kappa_1| > 1$ and $|\kappa_2| < 1$), then the point (u^*, v^*) is a saddle point.*
4. *If $|\kappa_1| = 1$ or $|\kappa_2| = 1$, then the point (u^*, v^*) is non-hyperbolic.*

Lemma 2.3. *[11, 13] Let $\mathrm{F}_{\mathcal{J}}(\kappa) = \kappa^2 - \mathrm{Tr}(\mathcal{J})\kappa + \det(\mathcal{J})$, where $\mathrm{F}_{\mathcal{J}}(1) > 0$ and κ_1 and κ_2 are the two roots of $\mathrm{F}_{\mathcal{J}}(\kappa) = 0$. Then,*

1. *$|\kappa_1| < 1$ and $|\kappa_2| < 1$ if and only if $\mathrm{F}_{\mathcal{J}}(-1) > 0$ and $\mathrm{F}_{\mathcal{J}}(0) < 1$.*
2. *$|\kappa_1| > 1$ and $|\kappa_2| > 1$ if and only if $\mathrm{F}_{\mathcal{J}}(-1) > 0$ and $\mathrm{F}_{\mathcal{J}}(0) > 1$.*
3. *$|\kappa_1| < 1$ and $|\kappa_2| > 1$ (or $|\kappa_1| > 1$ and $|\kappa_2| < 1$) if and only if $\mathrm{F}_{\mathcal{J}}(-1) < 0$.*
4. *$\kappa_1 = -1$ and $|\kappa_2| \neq 1$ if and only if $\mathrm{F}_{\mathcal{J}}(-1) = 0$ and $\mathrm{Tr}(\mathcal{J}) \neq 0, 2$.*
5. *κ_1 and κ_2 are complex numbers and $|\kappa_1| = |\kappa_2| = 1$ if and only if $\mathrm{Tr}(\mathcal{J})^2 - 4\det(\mathcal{J}) < 0$ and $\mathrm{F}_{\mathcal{J}}(0) = 1$.*

Lemma 2.4. *[14] Assume that $X_{k+1} = G_s(U_k)$ is an n-dimensional discrete dynamical system where $s \in R$ is a bifurcation parameter. Let X^* be a fixed point of H_s and suppose that the characteristic equation of the Jacobian matrix $M_J(U^*) = (\beta_{ij})_{n\times n}$ of n-dimensional map $G_s(X_k)$ is expressed as*

$$\mathrm{F}_{\mathcal{J}}(\kappa) = \kappa^n + \beta_1\kappa^{n-1} + \cdots + \beta_{n-1}\kappa + \beta_n, \tag{2.2}$$

where $\beta_i = \beta_i(s,u)$, $i = 1,2,3,\cdots,n$, and u is a control parameter. Suppose that $\Delta_0^{\pm}(s,u) = 1$, and $\Delta_1^{\pm}(s,u),\cdots,\Delta_n^{\pm}(s,u)$ is a sequence of the determinants given by

$$\Delta_i^{\pm}(s,u) = \det(\Upsilon_1 \pm \Upsilon_2), \quad i = 1,2,\cdots,n, \tag{2.3}$$

where

$$\Upsilon_1 = \begin{pmatrix} 1 & \beta_1 & \beta_2 & \cdots & \beta_{i-1} \\ 0 & 1 & \beta_1 & \cdots & \beta_{i-2} \\ 0 & 0 & 1 & \cdots & \beta_{i-3} \\ \cdots & \cdots & \cdots & \cdots & \cdots \\ 0 & 0 & 0 & \cdots & 1 \end{pmatrix}, \ \Upsilon_2 = \begin{pmatrix} \beta_{n-i+1} & \beta_{n-i+2} & \cdots & \beta_{n-1} & \beta_n \\ \beta_{n-i+2} & \beta_{n-i+3} & \cdots & \beta_n & 0 \\ \cdots & \cdots & \cdots & \cdots & \cdots \\ \beta_{n-1} & \beta_n & \cdots & 0 & 0 \\ \beta_n & 0 & 0 & \cdots & 0 \end{pmatrix}. \tag{2.4}$$

In addition, assume that the following propositions are true.

- ***C1-*** *Eigenvalue criterion:* $\mathrm{F}_{\mathcal{J}}(-1) = 0$, $\Delta_{n-1}^{\pm}(\omega,u) > 0$, $\mathrm{F}_{\mathcal{J}}(1) > 0$, $\Delta_i^{\pm}(\omega,u) > 0$, $i = n-2, n-4,\cdots,1$ *(or 1), when n is even (or odd), respectively.*
- ***C2-*** *Transversality criterion:* $\dfrac{\sum_{i=1}^{n}(-1)^{n-i}a_i'}{\sum_{i=1}^{n}(-1)^{n-i}(n-i+1)\beta_{i-1}} \neq 0$, *where β_i' represents the derivative of $a(s)$ at $s = \omega$. Then, a flip bifurcation exists at a critical value ω.*

3. Discretization of model (1.1)

The present section employs the fractional derivative of Caputo to discretize the continuous-time model (1.1). The objective of this part is to develop a discrete representation of the fractional-order system using the piecewise constant argument technique, which is equivalent to the techniques described in [11]. To accomplish this, we start with the following structures:

$$\begin{cases} {}_cD^{\gamma}x(t) = Rx\left(\left\lfloor\frac{t}{\omega}\right\rfloor\omega\right)\left(1 - x\left(\left\lfloor\frac{t}{\omega}\right\rfloor\omega\right)\right) - \dfrac{\delta x\left(\left\lfloor\frac{t}{\omega}\right\rfloor\omega\right)y\left(\left\lfloor\frac{t}{\omega}\right\rfloor\omega\right)}{f + x\left(\left\lfloor\frac{t}{\omega}\right\rfloor\omega\right)} - Mx\left(\left\lfloor\frac{t}{\omega}\right\rfloor\omega\right)^2, \\ {}_cD^{\gamma}y(t) = \dfrac{cx\left(\left\lfloor\frac{t}{\omega}\right\rfloor\omega\right)y\left(\left\lfloor\frac{t}{\omega}\right\rfloor\omega\right)}{f + x\left(\left\lfloor\frac{t}{\omega}\right\rfloor\omega\right)} - \dfrac{dx\left(\left\lfloor\frac{t}{\omega}\right\rfloor\omega\right)y\left(\left\lfloor\frac{t}{\omega}\right\rfloor\omega\right)}{f + x\left(\left\lfloor\frac{t}{\omega}\right\rfloor\omega\right)} - sy\left(\left\lfloor\frac{t}{\omega}\right\rfloor\omega\right). \end{cases}$$

Here, the discretization step size is represented by the parameter $\omega > 0$.

- For $t \in [0,\omega)$, we have $\frac{t}{\omega} \in [0,1)$. Therefore, the system becomes

$$\begin{cases} {}_cD^{\gamma}x(t) = Rx_0(1 - x_0) - \dfrac{\delta x_0 y_0}{f + x_0} - Mx_0^2, \\ {}_cD^{\gamma}y(t) = \dfrac{cx_0y_0}{f + x_0} - \dfrac{dx_0y_0}{f + x_0} - sy_0. \end{cases} \tag{3.1}$$

Next, system (3.1) can be written as

$$\begin{cases} x_1(t) = x_0 + \dfrac{\omega^\gamma}{\Gamma(\gamma+1)}\left(Rx_0\,(1-x_0) - \dfrac{\delta x_0 y_0}{f+x_0} - Mx_0^2\right), \\ y_1(t) = y_0 + \dfrac{\omega^\gamma}{\Gamma(\gamma+1)}\left(\dfrac{cx_0y_0}{f+x_0} - \dfrac{dx_0y_0}{f+x_0} - sy_0\right). \end{cases}$$

- For $t \in [\omega, 2\omega)$, we have $\frac{t}{\omega} \in [1, 2)$. Thus, the system turns as

$$\begin{cases} {}_cD^\gamma x(t) = Rx_1(1-x_1) - \dfrac{\delta x_1 y_1}{f+x_1} - Mx_1^2, \\ {}_cD^\gamma y(t) = \dfrac{cx_1y_1}{f+x_1} - \dfrac{dx_1y_1}{f+x_1} - sy_1. \end{cases}$$

The solution to this system can be expressed as

$$\begin{cases} x_2(t) = x_1(\omega) + \dfrac{\omega^\gamma}{\Gamma(\gamma+1)}\left(Rx_1(\omega)\,(1-x_1(\omega)) - \dfrac{\delta x_1(\omega)y_1(\omega)}{f+x_1(\omega)} - Mx_1(\omega)^2\right), \\ y_2(t) = y_1(\omega) + \dfrac{\omega^\gamma}{\Gamma(\gamma+1)}\left(\dfrac{cx_1(\omega)y_1(\omega)}{f+x_1(\omega)} - \dfrac{dx_1(\omega)y_1(\omega)}{f+x_1(\omega)} - sy_1(\omega)\right). \end{cases}$$

- For $t \in [2\omega, 3\omega)$, it follows that $\frac{t}{\omega} \in [2, 3)$. Therefore, the system can be written as

$$\begin{cases} {}_cD^\gamma x(t) = Rx_2(1-x_2) - \dfrac{\delta x_2 y_2}{f+x_2} - Mx_2^2, \\ {}_cD^\gamma y(t) = \dfrac{cx_2y_2}{f+x_2} - \dfrac{dx_2y_2}{f+x_2} - sy_2. \end{cases}$$

Hence, the solution of the system takes the form of

$$\begin{cases} x_3(t) = x_2(2\omega) + \dfrac{\omega^\gamma}{\Gamma(\gamma+1)}\left(Rx_2(2\omega)\,(1-x_2(2\omega)) - \dfrac{\delta x_2(2\omega)y_2(2\omega)}{f+x_2(2\omega)} - Mx_2(2\omega)^2\right), \\ y_3(t) = y_2(2\omega) + \dfrac{\omega^\gamma}{\Gamma(\gamma+1)}\left(\dfrac{cx_2(2\omega)y_2(2\omega)}{f+x_2(2\omega)} - \dfrac{dx_2(2\omega)y_2(2\omega)}{f+x_2(2\omega)} - sy_2(2\omega)\right). \end{cases}$$

- Implementing n iterations, the system turns to

$$\begin{cases} x_{n+1}(t) = x_n(n\omega) + \dfrac{\omega^\gamma}{\Gamma(\gamma+1)}\left(Rx_n(n\omega)\,(1-x_n(n\omega)) - \dfrac{\delta x_n(n\omega)y_n(n\omega)}{f+x_n(n\omega)} - Mx_n(n\omega)^2\right), \\ y_{n+1}(t) = y_n(n\omega) + \dfrac{\omega^\gamma}{\Gamma(\gamma+1)}\left(\dfrac{cx_n(n\omega)y_n(n\omega)}{f+x_n(n\omega)} - \dfrac{dx_n(n\omega)y_n(n\omega)}{f+x_n(n\omega)} - sy_n(n\omega)\right). \end{cases}$$

- As t approaches $(n+1)\,\omega$, the discretized version of system (1.1) becomes

$$\begin{cases} x_{n+1} = x_n + \dfrac{\omega^\gamma}{\Gamma(\gamma+1)}\left(Rx_n\,(1-x_n) - \dfrac{\delta x_n y_n}{f+x_n} - Mx_n^2\right), \\ y_{n+1} = y_n + \dfrac{\omega^\gamma}{\Gamma(\gamma+1)}\left(\dfrac{cx_ny_n}{f+x_n} - \dfrac{dx_ny_n}{f+x_n} - sy_n\right). \end{cases} \tag{3.2}$$

System (3.2) represents the discrete version of the continuous-time model (1.1).

4. Existence and local stability of the fixed points

In this part, we develop the stability of the fixed points of model (3.2). It is worth noting that the equilibria of system (3.2) are obtained by finding the solutions of the algebraic nonlinear system

$$\begin{cases} \left(Rx(1-x) - \dfrac{\delta xy}{f+x} - Mx^2\right) = 0, \\ \left(\dfrac{cxy}{f+x} - \dfrac{dxy}{f+x} - sy\right) = 0. \end{cases}$$

Since the parameters R, δ, f, M, c, d, and s are positive, model (3.2) has two fixed points $O = (0,0)$ and $\mathcal{E} = \left(\dfrac{R}{R+M}, 0\right)$. If $c > d + s$ and $R(c-d-s) > sf(R+M)$, system (3.2) has a unique positive fixed point which is

$$\mathcal{P} = \left(\frac{sf}{c-d-s}, \frac{f(c-d)(R(c-d-s) - sf(R+M))}{\delta(c-d-s)^2}\right). \tag{4.1}$$

The Jacobian matrix of system (3.2) at any fixed point $\mathcal{M} = (x, y)$ is expressed by

$$\mathcal{J}_{\mathcal{M}} = \begin{pmatrix} 1 + \dfrac{\omega^\gamma}{\Gamma(\gamma+1)}\left(R - 2x(R+M) - \dfrac{\delta fy}{(f+x)^2}\right) & -\left(\dfrac{\delta x\omega^\gamma}{(f+x)\Gamma(\gamma+1)}\right) \\ \dfrac{\omega^\gamma}{\Gamma(\gamma+1)}\left(\dfrac{fy(c-d)}{(f+x)^2}\right) & 1 + \dfrac{\omega^\gamma}{\Gamma(\gamma+1)}\left(\dfrac{x(c-d)}{f+x} - s\right) \end{pmatrix}, \tag{4.2}$$

whose characteristic equation is

$$\mathrm{F}_{\mathcal{J}}(\kappa) = \kappa^2 - \mathrm{Tr}(\mathcal{J})\kappa + \det(\mathcal{J}) = 0,$$

where

$$\begin{aligned} \mathrm{Tr}(\mathcal{J}) &= 2 + \frac{\omega^\gamma}{\Gamma(\gamma+1)}\left(R - s - 2x(R+M) - \frac{\delta fy}{(f+x)^2} + \frac{x(c-d)}{f+x}\right), \\ \det(\mathcal{J}) &= \left(1 + \frac{\omega^\gamma}{\Gamma(\gamma+1)}\left(R - 2x(R+M) - \frac{\delta fy}{(f+x)^2}\right)\right)\left(1 + \frac{\omega^\gamma}{\Gamma(\gamma+1)}\left(\frac{x(c-d)}{f+x} - s\right)\right) \\ &\quad + \frac{\omega^{2\gamma}}{(\Gamma(\gamma+1))^2}\left(\frac{\delta fxy(c-d)}{(f+x)^3}\right). \end{aligned}$$

The stability of the fixed points is then tested through Lemmas 2.2 and 2.3.

Theorem 4.1. *The trivial fixed point $O = (0,0)$ is a saddle point if $0 < \omega < \left(\frac{2\Gamma(\gamma+1)}{s}\right)^{\frac{1}{\gamma}}$, a source if $\omega > \left(\frac{2\Gamma(\gamma+1)}{s}\right)^{\frac{1}{\gamma}}$, and non-hyperbolic if $\omega = \left(\frac{2\Gamma(\gamma+1)}{s}\right)^{\frac{1}{\gamma}}$.*

Proof. The Jacobian matrix of system (3.2) at the trivial fixed point $O = (0,0)$ is

$$\mathcal{J}_O = \begin{pmatrix} \left(1 + \dfrac{R\omega^\gamma}{\Gamma(\gamma+1)}\right) & 0 \\ 0 & \left(1 - \dfrac{s\omega^\gamma}{\Gamma(\gamma+1)}\right) \end{pmatrix},$$

with

$$\kappa_1 = 1 + \frac{R\omega^\gamma}{\Gamma(\gamma+1)} > 1, \quad \kappa_2 = 1 - \frac{s\omega^\gamma}{\Gamma(\gamma+1)}.$$

Based on Lemma 2.2, we can determine that the fixed point $O = (0, 0)$ is a saddle if $0 < \omega < \left(\frac{2\Gamma(\gamma+1)}{s}\right)^{\frac{1}{\gamma}}$, a source if $\omega > \left(\frac{2\Gamma(\gamma+1)}{s}\right)^{\frac{1}{\gamma}}$, and non-hyperbolic if $\omega = \left(\frac{2\Gamma(\gamma+1)}{s}\right)^{\frac{1}{\gamma}}$.

□

Theorem 4.2. *For the semi-trivial fixed point $\mathcal{E} = \left(\frac{R}{R+M}, 0\right)$, we have the following results:*

- *When $R(c-d-s) < sf(R+M)$, we have*
  1. *$\mathcal{E}$ is locally asymptotically stable (sink) if $0 < \omega < \min\left\{\left(\frac{2\Gamma(\gamma+1)}{R}\right)^{1/\gamma}, \left(\frac{2\Gamma(\gamma+1)}{q_2}\right)^{1/\gamma}\right\}$.*
  2. *$\mathcal{E}$ is a source if $\omega > \max\left\{\left(\frac{2\Gamma(\gamma+1)}{R}\right)^{1/\gamma}, \left(\frac{2\Gamma(\gamma+1)}{q_2}\right)^{1/\gamma}\right\}$.*
  3. *$\mathcal{E}$ is a saddle if $\left(\frac{2\Gamma(\gamma+1)}{R}\right)^{1/\gamma} < \omega < \left(\frac{2\Gamma(\gamma+1)}{q_2}\right)^{1/\gamma}$ with eigenvalues $|\kappa_1| > 1$ and $|\kappa_2| < 1$, or $\left(\frac{2\Gamma(\gamma+1)}{q_2}\right)^{1/\gamma} < \omega < \left(\frac{2\Gamma(\gamma+1)}{R}\right)^{1/\gamma}$ with eigenvalues $|\kappa_1| < 1$ and $|\kappa_2| > 1$.*
  4. *$\mathcal{E}$ is non-hyperbolic if*

$$\omega = \left(\frac{2\Gamma(\gamma+1)}{R}\right)^{1/\gamma}, \quad or \quad \omega = \left(\frac{2\Gamma(\gamma+1)}{q_2}\right)^{1/\gamma}.$$

- *When $R(c-d-s) > sf(R+M)$, we have*
  1. *$\mathcal{E}$ is a source if $0 < \omega \left(\frac{2\Gamma(\gamma+1)}{R}\right)^{1/\gamma}$.*
  2. *$\mathcal{E}$ is a saddle if $\omega > \left(\frac{2\Gamma(\gamma+1)}{R}\right)^{1/\gamma}$.*
  3. *$\mathcal{E}$ is non-hyperbolic if*

$$\omega = \left(\frac{2\Gamma(\gamma+1)}{R}\right)^{1/\gamma}.$$

Proof. The Jacobian matrix $\mathcal{J}_\mathcal{E}$ of system (3.2) is shown as

$$\mathcal{J}_\mathcal{E} = \begin{pmatrix} \left(1 - \frac{R\omega^\gamma}{\Gamma(\gamma+1)}\right) & \frac{-q_1\omega^\gamma}{\Gamma(\gamma+1)} \\ 0 & \left(1 - \frac{q_2\omega^\gamma}{\Gamma(\gamma+1)}\right) \end{pmatrix}, \tag{4.3}$$

where

$$q_1 = \frac{\delta R}{f(R+M)+R}, \quad q_2 = \left(\frac{sf(R+M) - R(c-d-s)}{f(R+M)+R}\right).$$

Consequently, the eigenvalues are provided as follows:

$$\kappa_1 = \left(1 - \frac{R\omega^\gamma}{\Gamma(\gamma+1)}\right), \quad \kappa_2 = \left(1 - \frac{q_2\omega^\gamma}{\Gamma(\gamma+1)}\right).$$

Based on Lemma 2.2, we confirm the results of Theorem 4.2. □

Theorem 4.3. *For the unique positive fixed point $\mathcal{P}$ of system* (3.2)*, the following statements are true.*

1. *If any one of the following conditions holds, then $\mathcal{P}$ is locally asymptotically stable.*

$$i\text{-}\ \Delta < 0 \text{ and } 0 < \omega \leq \omega_0 = \left(\frac{H(c-d)\,\Gamma(\gamma+1)}{s(R(c-d-s)-s\,f(R+M))}\right)^{1/\gamma},$$

$$ii\text{-}\ \Delta \geq 0 \text{ and } 0 < \omega \leq \omega_1 = \left(\frac{H(c-d)\,\Gamma(\gamma+1)-\Gamma(\gamma+1)\,\sqrt{\Delta}}{s(R(c-d-s)-sf(R+M))}\right)^{\frac{1}{\gamma}}.$$

2. *If any one of the following conditions holds, then $\mathcal{P}$ is unstable.*

$$i\text{-}\ \Delta < 0 \text{ and } \omega > \omega_0 = \left(\frac{H(c-d)\,\Gamma(\gamma+1)}{s(R(c-d-s)-s\,f(R+M))}\right)^{1/\gamma},$$

$$ii\text{-}\ \Delta \geq 0 \text{ and } \omega > \omega_2 = \left(\frac{H(c-d)\,\Gamma(\gamma+1)+\Gamma(\gamma+1)\,\sqrt{\Delta}}{s(R(c-d-s)-sf(R+M))}\right)^{1/\gamma}.$$

3. *The fixed point $\mathcal{P}$ is unstable if*

$$\Delta \geq 0 \quad \text{and} \quad \omega_1 < \omega \leq \omega_2.$$

4. *The fixed point P_1 is non-hyperbolic if one of the following conditions holds.*

$$i\text{-}\ \Delta < 0 \text{ and } \omega = \omega_0 = \left(\frac{H(c-d)\,\Gamma(\gamma+1)}{s(R(c-d-s)-s\,f(R+M))}\right)^{1/\gamma},$$

$$ii\text{-}\ \Delta \geq 0 \text{ and } \omega = \omega_{1,2} = \left(\frac{H(c-d)\,\Gamma(\gamma+1)\mp\Gamma(\gamma+1)\,\sqrt{\Delta}}{s(R(c-d-s)-sf(R+M))}\right)^{1/\gamma} \text{ and } \omega \neq \left(\frac{2\Gamma(\gamma+1)}{H}\right)^{1/\gamma}.$$

Proof. We begin with the Jacobian matrix of system (3.2) at the coexistence fixed point $\mathcal{P}$ which is given by

$$\mathcal{J}_{\mathcal{P}} = \begin{pmatrix} 1-\dfrac{H\omega^{\gamma}}{\Gamma(\gamma+1)} & \dfrac{-s\delta\omega^{\gamma}}{(c-d)\Gamma(\gamma+1)} \\ \dfrac{(R(c-d-s)-sf(R+M))\omega^{\gamma}}{\delta\Gamma(\gamma+1)} & 1 \end{pmatrix},$$

where

$$H = \left(\frac{2sf(R+M)}{c-d-s}-\frac{s(R+f(R+M))}{c-d}\right).$$

Now, the auxiliary equation associated to $\mathcal{J}_{\mathcal{P}}$ is

$$\mathrm{F}_{\mathcal{J}}(\kappa) = \kappa^2 - \mathrm{T}r(\mathcal{J})\kappa + \mathrm{D}et(\mathcal{J}). \tag{4.4}$$

Here,

$$\mathrm{Tr}(\mathcal{J}) = 2-\frac{H\omega^{\gamma}}{\Gamma(\gamma+1)},$$

$$\det(\mathcal{J}) = 1-\frac{H\,\omega^{\gamma}}{\Gamma(\gamma+1)}+\frac{s\,(R(c-d-s)-sf(R+M))\,\omega^{2\gamma}}{(c-d)\Gamma(\gamma+1)^2}.$$

Utilizing the auxiliary equation, we have

$$\mathrm{F}_{\mathcal{J}}(1) = \frac{s\left(R(c-d-s) - sf(R+M)\right)\omega^{2\gamma}}{(c-d)\Gamma(\gamma+1)^2} > 0, \quad \mathrm{F}_{\mathcal{J}}(0) = \det(\mathcal{J}),$$
$$\mathrm{F}_{\mathcal{J}}(-1) = 4 - \frac{2H\,\omega^{\gamma}}{\Gamma(\gamma+1)} + \frac{s\left(R(c-d-s) - sf(R+M)\right)\omega^{2\gamma}}{(c-d)\Gamma(\gamma+1)^2}.$$

The discriminant of equation $\mathrm{F}_{\mathcal{J}}(\kappa) = 0$ is expressed as

$$\Delta = H^2(c-d)^2 - 4s(c-d)(R(c-d-s) - sf(R+M)).$$

From Lemma 2.3, it can be guaranteed that the coexistence fixed point satisfies the results of Theorem 4.3. □

5. Neimark-Sacker bifurcation analysis

We here examine the Neimark-Sacker bifurcation by considering ω as the key control parameter. The relevant parameter space is specified as

$$\mathrm{B}_{NS} = \left\{(R, \delta, f, c, d, s, \gamma, \omega) \in R^8 \mid \Delta < 0 \text{ and } \omega = \omega_0 = \left(\frac{H(c-d)\,\Gamma(\gamma+1)}{s(R(c-d-s) - s\,f(R+M))}\right)^{1/\gamma}\right\}.$$

In order to further analyze the bifurcation behavior, we propose a small perturbation ω^* to the bifurcation parameter ω. This perturbation converts the system stated in model (3.2) into the following structure:

$$\begin{cases} x_{n+1} = x_n + \dfrac{(\omega+\omega^*)^{\gamma}}{\Gamma(\gamma+1)}\left(Rx_n(1-x_n) - \dfrac{\delta x_n y_n}{f+x_n} - Mx_n^2\right) = G_1(x_n, y_n), \\ y_{n+1} = y_n + \dfrac{(\omega+\omega^*)^{\gamma}}{\Gamma(\gamma+1)}\left(\dfrac{cx_n y_n}{f+x_n} - \dfrac{dx_n y_n}{f+x_n} - sy_n\right) = G_2(x_n, y_n). \end{cases} \tag{5.1}$$

We next consider $Z_n = x_n - x^*$ and $K_n = y_n - y^*$ as the deviations from the fixed point $\mathcal{P}$. To modify the perturbed system in model (5.1), we relocate the origin to $(0, 0)$ and perform a third-order Taylor series expansion to the nonlinear functions G_1 and G_2.

$$\begin{cases} Z_{n+1} = \beta_{11}Z_n + \beta_{12}K_n + \beta_{13}Z_n^2 + \beta_{14}Z_nK_n + \beta_{15}K_n^2 + \beta_{16}Z_n^3 + \beta_{17}Z_n^2K_n \\ \qquad + \beta_{18}Z_nK_n^2 + \beta_{19}K_n^3 + \mathcal{R}(\|(Z_n, K_n)\|^4), \\ K_{n+1} = \beta_{21}Z_n + \beta_{22}K_n + \beta_{23}Z_n^2 + \beta_{24}Z_nK_n + \beta_{25}K_n^2 + \beta_{26}Z_n^3 + \beta_{27}Z_n^2K_n \\ \qquad + \beta_{28}Z_nK_n^2 + \beta_{29}K_n^3 + \mathcal{R}(\|(Z_n, K_n)\|^4). \end{cases} \tag{5.2}$$

The coefficients are provided by

$$\beta_{11} = 1 - \frac{\omega^{\gamma}}{\Gamma(\gamma+1)}\left(\frac{2sf(R+M)}{c-d-s} - \frac{s(R+f(R+M))}{c-d}\right), \quad \beta_{12} = \frac{-s\delta\omega^{\gamma}}{(c-d)\Gamma(\gamma+1)}, \quad \beta_{22} = 1,$$
$$\beta_{21} = \frac{(R(c-d-s) - sf(R+M))\omega^{\gamma}}{\delta\Gamma(\gamma+1)}, \ \beta_{13} = \frac{\omega^{\gamma}}{\Gamma(\gamma+1)}\left(-2R + \frac{2\delta y^{*} f}{(f+x^{*})^{3}} - 2M\right), \ \beta_{15} = 0,$$
$$\beta_{14} = \frac{\omega^{\gamma}}{\Gamma(\gamma+1)}\left(-\frac{\delta x^{*}}{f+x^{*}}\right), \quad \beta_{16} = \frac{\omega^{\gamma}}{\Gamma(\gamma+1)}\left(-\frac{6\delta y^{*} f}{(f+x^{*})^{4}}\right), \quad \beta_{17} = \frac{\omega^{\gamma}}{\Gamma(\gamma+1)}\left(\frac{2\delta f}{(f+x^{*})^{3}}\right),$$
$$\beta_{23} = \frac{\omega^{\gamma}}{\Gamma(\gamma+1)}\left(-\frac{2(c-d)y^{*} f}{(f+x^{*})^{3}}\right), \ \beta_{24} = \frac{\omega^{\gamma}}{\Gamma(\gamma+1)}\left(\frac{(c-d)f}{(f+x^{*})^{2}}\right), \ \beta_{26} = \frac{\omega^{\gamma}}{\Gamma(\gamma+1)}\left(\frac{6(c-d)y^{*} f}{(f+x^{*})^{4}}\right),$$
$$\beta_{27} = \frac{\omega^{\gamma}}{\Gamma(\gamma+1)}\left(-\frac{2(c-d)f}{(f+x^{*})^{3}}\right), \quad \beta_{19} = \beta_{25} = \beta_{28} = \beta_{29} = 0.$$

The characteristic equation for system (5.2) computed at the origin can be expressed as

$$\mathrm{F}_{\mathcal{J}}(\kappa) = \kappa^{2} - \mathrm{T}r(\mathcal{J})_{\omega^{*}}\kappa + \mathrm{D}et(\mathcal{J})_{\omega^{*}}, \tag{5.3}$$

with

$$\mathrm{Tr}(\mathcal{J})_{\omega^{*}} = 2 - \frac{H(\omega+\omega^{*})^{\gamma}}{\Gamma(\gamma+1)},$$
$$\det(\mathcal{J})_{\omega^{*}} = 1 - \frac{H\,(\omega+\omega^{*})^{\gamma}}{\Gamma(\gamma+1)} + \frac{s\,(R(c-d-s) - sf(R+M))\,(\omega+\omega^{*})^{2\gamma}}{(c-d)\Gamma(\gamma+1)^{2}}.$$

In Eq (5.3), a pair of complex conjugate eigenvalues are shown as

$$\kappa_{1,2}(\omega^{*}) = \frac{\mathrm{Tr}(\mathcal{J})_{\omega^{*}} \mp i\sqrt{4\det(\mathcal{J})_{\omega^{*}} - \mathrm{Tr}(\mathcal{J})^{2}_{\omega^{*}}}}{2}.$$

Because the parameters are $(R, \delta, f, c, d, s, \gamma, \omega_0) \in \mathrm{B}_{NS}$, it follows that $|\kappa_{1,2}(0)| = 1$, and

$$\left.\frac{d|\kappa_{1,2}(\omega)|}{d\omega}\right|_{\omega=0} = \frac{\gamma H}{\Gamma(\gamma+1)}\left(\frac{H(c-d)\,\Gamma(\gamma+1)}{s(R(c-d-s) - s\,f(R+M))}\right)^{(\gamma-1)/\gamma} \neq 0.$$

The Neimark-Sacker bifurcation occurs when $\kappa^{j}_{1,2} \neq 1$ for $j = 1, 2, 3, 4$ and $\omega = 0$. This condition can be correspondingly formulated as:

$$\mathrm{Tr}(\mathcal{J})_{0} \neq -2, 0, 1, 2.$$

Using the coordinate transformation,

$$\begin{pmatrix} Z_n \\ K_n \end{pmatrix} = \begin{pmatrix} \beta_{12} & 0 \\ \mathcal{R} - \beta_{11} & -\mathcal{I} \end{pmatrix}\begin{pmatrix} \bar{x}_n \\ \bar{y}_n \end{pmatrix},$$

where the real part is $\mathcal{R} = \dfrac{\mathrm{Tr}(\mathcal{J})_{0}}{2}$ and the imaginary part is $\mathcal{I} = \dfrac{\sqrt{4\det(\mathcal{J})_{0} - \mathrm{Tr}(\mathcal{J})^{2}_{0}}}{2}$. System (5.2) is shifted into the equations

$$\begin{cases} \bar{x}_{n+1} = \mathcal{R}\bar{x}_n - \mathcal{I}\bar{y}_n + \tilde{G}_1(\bar{x}_n, \bar{y}_n), \\ \bar{y}_{n+1} = \mathcal{I}\bar{x}_n + \mathcal{R}\bar{y}_n + \tilde{G}_2(\bar{x}_n, \bar{y}_n). \end{cases} \tag{5.4}$$

Here,

$$\tilde{G}_1(\bar{x}_n, \bar{y}_n) = \frac{\beta_{13}}{\beta_{12}}Z^2 + \frac{\beta_{14}}{\beta_{12}}ZK + \frac{\beta_{15}}{\beta_{12}}K^2 + \frac{\beta_{16}}{\beta_{12}}Z^3 + \frac{\beta_{17}}{\beta_{12}}Z^2K + \frac{\beta_{18}}{\beta_{12}}ZK^2 + \frac{\beta_{19}}{\beta_{12}}K^3 + \bar{O}(\|(Z_n, K_n)\|^4),$$

$$\begin{aligned}\tilde{G}_2(\bar{x}_n, \bar{y}_n) = &\left(\frac{\beta_{13}(\mathcal{R}-\beta_{11})}{\mathcal{I}\beta_{12}} - \frac{\beta_{23}}{\mathcal{I}}\right)Z^2 + \left(\frac{\beta_{14}(\mathcal{R}-\beta_{11})}{\mathcal{I}\beta_{12}} - \frac{\beta_{24}}{\mathcal{I}}\right)ZK + \left(\frac{\beta_{15}(\mathcal{R}-\beta_{11})}{\mathcal{I}\beta_{12}} - \frac{\beta_{25}}{\mathcal{I}}\right)K^2 \\ &+ \left(\frac{\beta_{16}(\mathcal{R}-\beta_{11})}{\mathcal{I}\beta_{12}} - \frac{\beta_{26}}{\mathcal{I}}\right)Z^3 + \left(\frac{\beta_{17}(\mathcal{R}-\beta_{11})}{\mathcal{I}\beta_{12}} - \frac{\beta_{27}}{\mathcal{I}}\right)Z^2K + \left(\frac{\beta_{18}(\mathcal{R}-\beta_{11})}{\mathcal{I}\beta_{12}} - \frac{\beta_{28}}{\mathcal{I}}\right)ZK^2 \\ &+ \left(\frac{\beta_{19}(\mathcal{R}-\beta_{11})}{\mathcal{I}\beta_{12}} - \frac{\beta_{29}}{\mathcal{I}}\right)K^3 + \bar{O}(\|(Z_n, K_n)\|^4).\end{aligned}$$

Notice that the variables Z_n and K_n are presented as

$$Z = \beta_{12}\bar{x}_n, \quad K = (\mathcal{R}-\beta_{11})\bar{x}_n - \mathcal{I}\bar{y}_n.$$

A Neimark-Sacker bifurcation in system (5.4) requires a nonzero discriminatory quantity which is

$$\mathrm{L} = \left(\mathrm{Re}(\kappa_2 e_{21}) - \mathrm{Re}\left(\frac{(1-2\kappa_1)(\kappa_2)^2}{1-\kappa_1}e_{20}e_{11}\right) - \frac{1}{2}|e_{11}|^2 - |e_{02}|^2\right)_{\omega^*=0}. \tag{5.5}$$

If $\mathrm{L} < 0$, then the fixed point $\mathcal{P}$ undergoes a bifurcation resulting in an attracting invariant closed curve for $\omega^* > 0$. Conversely, if $\mathrm{L} > 0$, a repelling invariant closed curve bifurcates from the fixed point for $\omega^* < 0$, where

$$\begin{aligned}
e_{20} &= \frac{1}{8}\left[\frac{\partial^2\tilde{G}_1}{\partial\bar{x}^2} - \frac{\partial^2\tilde{G}_1}{\partial\bar{y}^2} + 2\frac{\partial^2\tilde{G}_2}{\partial\bar{x}\partial\bar{y}} + i\left(\frac{\partial^2\tilde{G}_2}{\partial\bar{x}^2} - \frac{\partial^2\tilde{G}_2}{\partial\bar{y}^2} - 2\frac{\partial^2\tilde{G}_1}{\partial\bar{x}\partial\bar{y}}\right)\right]\Bigg|_{\omega^*=0}, \\
e_{11} &= \frac{1}{4}\left[\frac{\partial^2\tilde{G}_1}{\partial\bar{x}^2} + \frac{\partial^2\tilde{G}_1}{\partial\bar{y}^2} + i\left(\frac{\partial^2\tilde{G}_2}{\partial\bar{x}^2} + \frac{\partial^2\tilde{G}_2}{\partial\bar{y}^2}\right)\right]\Bigg|_{\omega^*=0}, \\
e_{02} &= \frac{1}{8}\left[\frac{\partial^2\tilde{G}_1}{\partial\bar{x}^2} - \frac{\partial^2\tilde{G}_1}{\partial\bar{y}^2} - 2\frac{\partial^2\tilde{G}_2}{\partial\bar{x}\partial\bar{y}} + i\left(\frac{\partial^2\tilde{G}_2}{\partial\bar{x}^2} - \frac{\partial^2\tilde{G}_2}{\partial\bar{y}^2} + 2\frac{\partial^2\tilde{G}_1}{\partial\bar{x}\partial\bar{y}}\right)\right]\Bigg|_{\omega^*=0}, \\
e_{21} &= \frac{1}{16}\left[\frac{\partial^3\tilde{G}_1}{\partial\bar{x}^3} + \frac{\partial^3\tilde{G}_1}{\partial\bar{x}\partial\bar{y}^2} + \frac{\partial^3\tilde{G}_2}{\partial\bar{x}^2\partial\bar{y}} + \frac{\partial^3\tilde{G}_2}{\partial\bar{y}^3} + i\left(\frac{\partial^3\tilde{G}_2}{\partial\bar{x}^3} + \frac{\partial^3\tilde{G}_2}{\partial\bar{x}\partial\bar{y}^2} - \frac{\partial^3\tilde{G}_1}{\partial\bar{x}^2\partial\bar{y}} - \frac{\partial^3\tilde{G}_1}{\partial\bar{y}^3}\right)\right]\Bigg|_{\omega^*=0}.
\end{aligned}$$

Based on these findings, the following theorem is established.

Theorem 5.1. *If condition* $\mathrm{L} \neq 0$ *is satisfied, then system* (3.2) *exhibits a Neimark-Sacker bifurcation at the positive fixed point* $\mathcal{P}$ *as the bifurcation parameter* ω *crosses the critical value* B_{NS}. *The sign of* L *determines the type of bifurcation.*

- *For* $\mathrm{L} < 0$, *the system undergoes a subcritical Neimark-Sacker bifurcation, producing a stable invariant closed curve encircling* $\mathcal{P}$.
- *For* $\mathrm{L} > 0$, *a supercritical Neimark-Sacker bifurcation arises, producing an unstable invariant closed curve in the vicinity of the fixed point.*

6. Flip bifurcation analysis

We now use Lemma (2.4) to explore the flip bifurcation of system (3.2) for parameter perturbations constrained to the neighborhood of $\mathrm{B}_F^{1,2}$, where

$$\mathrm{B}_F^{1,2} = \left\{ \begin{array}{l} (R,\delta,f,c,d,s,\gamma,\omega) \in R^8 \mid \Delta < 0,\ \omega = \omega_{1,2} = \left(\dfrac{H(c-d)\,\Gamma(\gamma+1) \mp \Gamma(\gamma+1)\,\sqrt{\Delta}}{s(R(c-d-s) - s\,f(R+M))} \right)^{1/\gamma}, \\ \\ \quad \Delta = H^2(c-d)^2 - 4s(c-d)(R(c-d-s) - sf(R+M)) \text{ and } \omega \neq \left(\dfrac{2\Gamma(\gamma+1)}{H} \right)^{1/\gamma} \end{array} \right\}.$$

Theorem 6.1. *System* (3.2) *exhibits a flip bifurcation at the unique positive fixed point $\mathcal{P}$ provided that the following conditions are satisfied:*

$$\begin{aligned} 1 + \det(\mathcal{J}) &> 0, \\ 1 + \mathrm{Tr}(\mathcal{J}) + \det(\mathcal{J}) &= 0, \\ 1 - \mathrm{Tr}(\mathcal{J}) + \det(\mathcal{J}) &> 0. \end{aligned} \tag{6.1}$$

Consequently, a flip bifurcation forms at q when the parameters $(\alpha, \beta, q, \kappa)$ vary in a neighborhood of the set $\mathrm{B}_F^{1,2}$.

Proof. Using Lemmas 2.4 and 4.3 in combination, and evaluating the characteristic Eq (4.4) of system (3.2) at the equilibrium $\mathcal{P}$, we arrive at the following conditions:

$$\begin{aligned} &\Delta_0^{\mp}(q) = 1 > 0, \\ &\Delta_1^{+}(q) = 1 + \det(\mathcal{J}) > 0, \\ &(-1)^2 \mathrm{F}_{\mathcal{J}}(-1) = 1 + \mathrm{Tr}(\mathcal{J}) + \det(\mathcal{J}) = 0, \\ &\mathrm{F}_{\mathcal{J}}(1) = 1 - \mathrm{Tr}(\mathcal{J}) + \det(\mathcal{J}) > 0, \end{aligned}$$

which are satisfied precisely when

$$\omega = \omega_{1,2} = \left(\frac{H(c-d)\,\Gamma(\gamma+1) \mp \Gamma(\gamma+1)\,\sqrt{H^2(c-d)^2 - 4s(c-d)(R(c-d-s) - sf(R+M))}}{s(R(c-d-s) - s\,f(R+M))} \right)^{1/\gamma},$$

where

$$H = \left(\frac{2sf(R+M)}{c-d-s} - \frac{s(R+f(R+M))}{c-d} \right).$$

In addition, the transversality requirement takes the form

$$\frac{\mathrm{Tr}(\mathcal{J})' + \det(\mathcal{J})'}{\mathrm{Tr}(\mathcal{J}) + 2} \neq 0,$$

where

$$\mathrm{Tr}(\mathcal{J})' = \left. \frac{\mathrm{dTr}(\mathcal{J})}{\mathrm{d}\omega} \right|_{\omega=\omega_{1,2}}, \quad \det(\mathcal{J})' = \left. \frac{\mathrm{d}\det(\mathcal{J})}{dq} \right|_{q=q_{1,2}}.$$

Hence, system (3.2) encounters a flip bifurcation at the two critical values $\omega = \omega_1$ and $\omega = \omega_2$. □

7. Controlling the chaos

Chaos is an essential feature of nonlinear dynamical systems. It occurs in discrete-time models, such as difference equations and iterative maps, when tiny changes in initial conditions cause unexpected long-term behavior. Although chaotic dynamics are potentially beneficial in fields such as cryptography and optimization, they frequently provide difficulties in areas such as ecology, engineering, medicine, and economics, where predictable and consistent behavior is needed. Various strategies have been suggested for this objective, among them the Ott–Grebogi–Yorke (OGY) approach [15], feedback control [16], and others [17]. We here adopt a hybrid control approach [18] to control chaos in system (3.2). To carry this out, the controlled system is initially expressed in the manner

$$\begin{cases} x_{n+1} = \xi\left(x_n + \dfrac{\omega^\gamma}{\Gamma(\gamma+1)}\left(Rx_n\left(1-x_n\right) - \dfrac{\delta x_n y_n}{f+x_n} - Mx_n^2\right)\right) + (1-\xi)\, x_n, \\ y_{n+1} = \xi\left(y_n + \dfrac{\omega^\gamma}{\Gamma(\gamma+1)}\left(\dfrac{cx_n y_n}{f+x_n} - \dfrac{dx_n y_n}{f+x_n} - sy_n\right)\right) + (1-\xi)\, y_n. \end{cases} \tag{7.1}$$

Note that the parameter $0 < \xi < 1$ is considered as a control variable in the hybrid control scheme. The Jacobian matrix of model (7.1) is then shown by

$$\mathcal{J}^c_{\mathcal{P}} = \begin{pmatrix} 1 - \dfrac{H\,\xi\,\omega^\gamma}{\Gamma(\gamma+1)} & \dfrac{-s\delta\,\xi\,\omega^\gamma}{(c-d)\Gamma(\gamma+1)} \\ \dfrac{(R(c-d-s) - sf(R+M))\,\xi\,\omega^\gamma}{\delta\Gamma(\gamma+1)} & 1 \end{pmatrix},$$

where

$$H = \left(\frac{2sf(R+M)}{c-d-s} - \frac{s(R+f(R+M))}{c-d}\right).$$

This gives us

$$\kappa^2 - \mathrm{T}r(\mathcal{J}^c)\kappa + \mathrm{D}et(\mathcal{J}^c) = 0, \tag{7.2}$$

where

$$\begin{aligned} \mathrm{Tr}(\mathcal{J}) &= 2 - \frac{H\,\xi\,\omega^\gamma}{\Gamma(\gamma+1)}, \\ \mathrm{D}et(\mathcal{J}) &= 1 - \frac{H\,\xi\,\omega^\gamma}{\Gamma(\gamma+1)} + \frac{s\left(R(c-d-s) - sf(R+M)\right)\,\xi^2\,\omega^{2\gamma}}{(c-d)\Gamma(\gamma+1)^2}. \end{aligned}$$

Lemma 7.1. *Suppose that $c > d+s$ and $R(c-d-s) > sf(R+M)$. Then, the unique positive fixed point*

$$\mathcal{P} = \left(\frac{sf}{c-d-s}, \frac{f(c-d)(R(c-d-s) - sf(R+M))}{\delta(c-d-s)^2}\right)$$

of model (7.1) *is locally asymptotically stable provided that the condition*

$$\left|2 - \frac{H\,\xi\,\omega^\gamma}{\Gamma(\gamma+1)}\right| < 2 - \frac{H\,\xi\,\omega^\gamma}{\Gamma(\gamma+1)} + \frac{s\left(R(c-d-s) - sf(R+M)\right)\,\xi^2\,\omega^{2\gamma}}{(c-d)\Gamma(\gamma+1)^2} < 2 \tag{7.3}$$

holds.

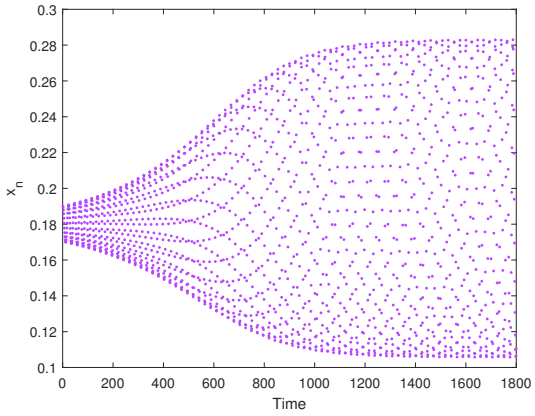

(a) Unstable solution for x_n in system (3.2) when $\omega = 0.092$.

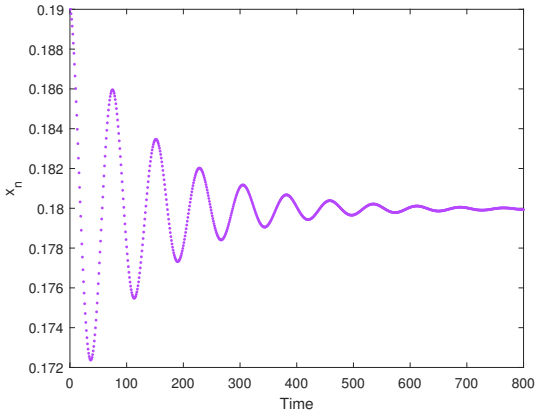

(b) Stable solution for x_n in controlling system (3.2) when $\omega = 0.092$ and $\xi = 0.9$.

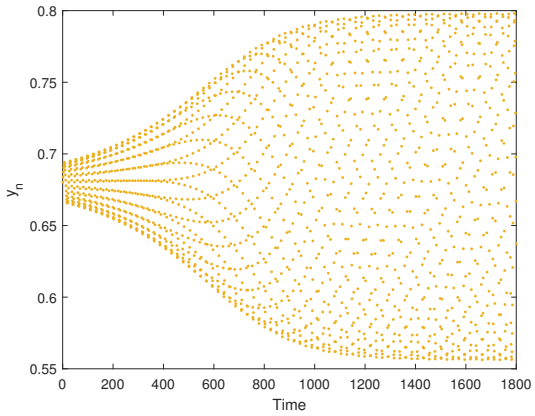

(c) Unstable solution for y_n in system (3.2) when $\omega = 0.092$.

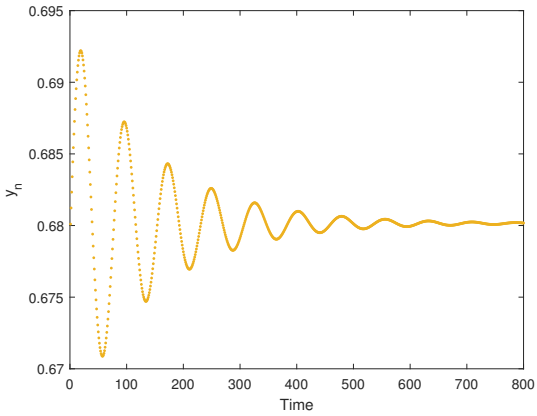

(d) Stable solution for y_n in controlling system (3.2) when $\omega = 0.092$ and $\xi = 0.9$.

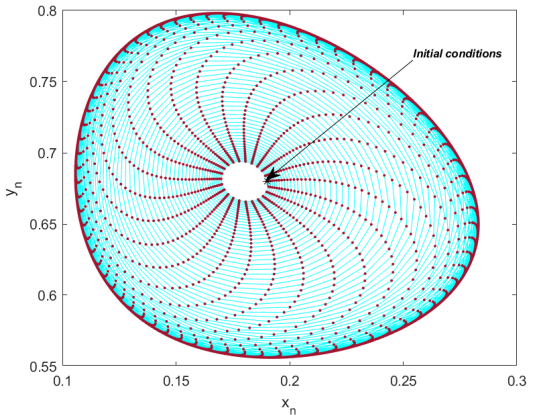

(e) Phase portrait for $\omega = 0.092$.

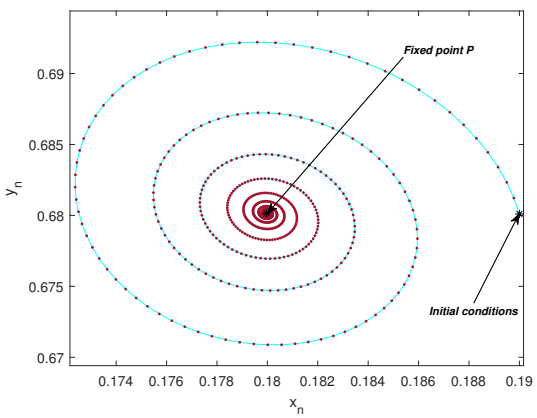

(f) Phase portrait for $\omega = 0.0247$ and $\xi = 0.9$.

Figure 1. The phase portraits and time series of systems (3.2) and (7.1) for different values of ω are presented as follows: (a, c, e) $\omega = 0.092$; (b, d, f) $\omega = 0.092$; and $\xi = 0.9$, respectively, with parameter values $R = 5.23$, $\delta = 5.895$, $f = 0.798$, $M = 1.05$, $c = 6.798$, $d = 3.13$, $s = 0.675$, and $\gamma = 0.75$.

Example 7.2. *This example explains how a hybrid control strategy can stabilize the system under discussion. We use the parameters* $R = 5.23$, $\delta = 5.895$, $f = 0.798$, $M = 1.05$, $c = 6.798$, $d = 3.13$, $s = 0.675$, $\gamma = 0.75$, *and the initial condition* $(0.19, 0.64)$. *Figure 1 depicts that the positive fixed point* $\mathcal{P}$ *is unstable (Figures 1(a),(c)), and the trajectories evolve toward a closed invariant curve (Figure 1(e)). When we apply the hybrid control technique,* $\mathcal{P}$ *turns out to be stable (Figures 1(b),(d)), while the closed invariant curve disappears (Figure 1(f)). This definitely illustrates how hybrid control efficiently stabilizes the system and removes chaotic behavior.*

8. Numerical simulations

Numerical simulations are implemented in this part to demonstrate the dynamics of the proposed model under various parameter values. These simulations, which are executed in MATLAB, are employed to confirm the mathematical findings gained in earlier sections.

Example 8.1. *We address the behavior of system* (3.2) *when it encounters a Neimark-Sacker bifurcation. Most notably, we explore system* (3.2) *for the values of parameters* $R = 5.23$, $\delta = 5.895$, $f = 0.798$, $M = 1.05$, $c = 6.798$, $d = 3.13$, $s = 0.675$, $\gamma = 0.5$, *and* $\omega \in [0, 0.1849]$, *and initial conditions* $I_0' = (0.12, 0.72)$. *Considering* ω *as the bifurcation parameter, we observed that at* $\omega_0 = 0.0217$, *the positive fixed point* $\mathcal{P}$ *becomes unstable, resulting in a Neimark-Sacker bifurcation. The Jacobian matrix for* $\mathcal{P}$ *is presented by*

$$J(E) = \begin{pmatrix} 0.9375 & -0.1805 \\ 0.34641.0000 & \end{pmatrix},$$

where the associated characteristic polynomial is given by

$$\mathcal{F}_{\mathcal{J}}(\kappa) = \kappa^2 - 1.9375\,\kappa + 1. \tag{8.1}$$

Here, the eigenvalues are $\kappa_1 = 0.9687 - 0.2481\,i$ *and* $\kappa_2 = 0.9687 + 0.2481\,i$, *satisfying* $|\kappa_{1,2}| = 1$. *The discriminatory quantity in the present situation is* $\mathrm{L} = -0.23421$, *fulfilling the requirements outlined in Theorem 5.1. The bifurcation diagrams of* x_n *and* y_n, *along with their associated maximum Lyapunov exponents (MLE), are illustrated in Figure 2 for the assigned parameter set. Moreover, Figures 2(a),(b) exhibit the stability of the positive fixed point* $\mathcal{P}$ *for* $0 < \omega < 0.0217$. *Note that the fixed point loses stability at* $\omega_0 = 0.0217$, *and the point E becomes unstable at* $0.0217 < \omega < 0.1849$. *Hence, the Neimark-Sacker bifurcation generates a closed invariant curve around the fixed point* $\mathcal{P}$. *It is worth noting that Figure 2(c) demonstrates that when* ω *increases, so does the size of this invariant curve, which is accompanied by positive maximum Lyapunov exponents. In Figures 3 and 4, we depict the phase portraits and related time series of* x_n *for system* (3.2) *with bifurcation parameters* $\omega = 0.0129$, 0.0217, 0.0247, 0.178, *and* 0.1849. *When* $0 < h < 0.1443$, *all trajectories converge to the fixed point* $\mathcal{P}$, *which stays stable as illustrated in Figures 3(a),(d). However, the fixed point* $\mathcal{P}$ *loses stability for* $0.0217 \leq h < 0.1849$. *This leads to an attracting closed invariant curve encircling* $\mathcal{P}$, *toward which all trajectories converge (see Figures 3(c)–(f)). Finally, considering* $h = 0.189$, *the system undergoes a transition to chaos and chaotic attractors appear, as depicted in Figure 4.*

From an environmental standpoint, this type of bifurcation represents a loss of stability of a fixed point and the appearance of long-term oscillations along a closed invariant curve, which frequently take the form of quasi-periodic cycles that have the potential to eventually result in chaotic dynamics or frequency locking. In phytoplankton-zooplankton systems, such a bifurcation typically indicates a shift from steady co-existence to ongoing, and sometimes complex, population cycles, with significant implications for bloom formation, grazing regulation, and the predictability of ecosystem dynamics.

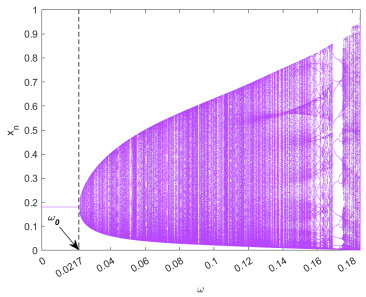

(a) Bifurcation diagram for x_n.

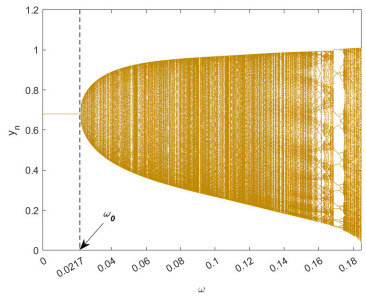

(b) Bifurcation diagram for y_n.

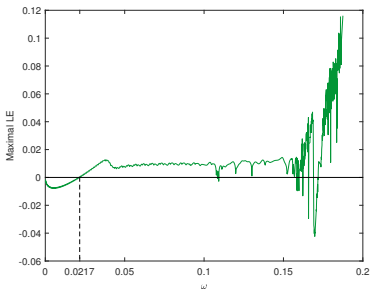

(c) Maximum Lyapunov exponents.

Figure 2. (a),(b) Neimark-Sacker bifurcation diagram of system (3.2). (c) Corresponding maximum Lyapunov exponents for the parameter values: $R = 5.23$, $\delta = 5.895$, $f = 0.798$, $M = 1.05$, $c = 6.798$, $d = 3.13$, $s = 0.675$, $\gamma = 0.5$, and $\omega \in [0, 0.1849]$.

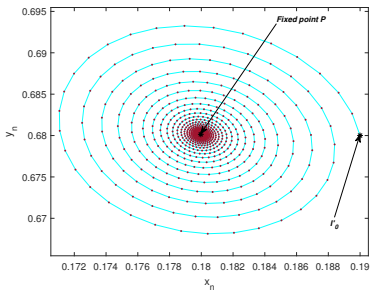

(a) Phase portrait for $\omega = 0.0129$.

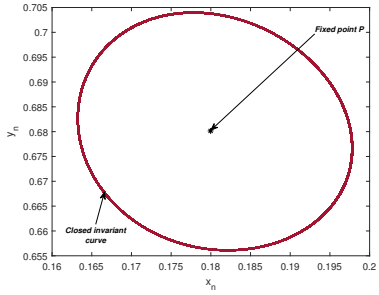

(b) Phase portrait for $\omega = 0.0217$.

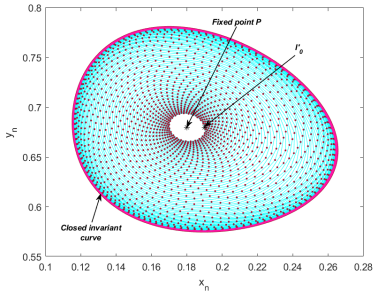

(c) Phase portrait for $\omega = 0.0247$.

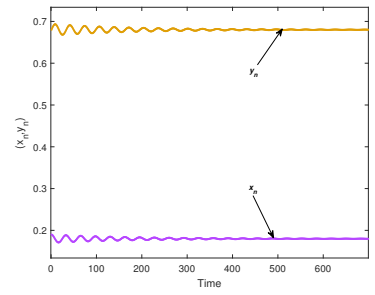

(d) Time evolution for 0.0129.

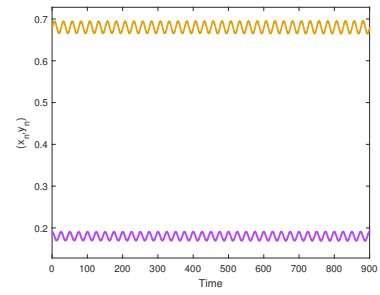

(e) Time evolution for 0.0217.

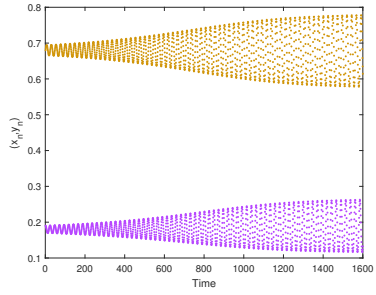

(f) Time evolution for 0.0247.

Figure 3. Phase portraits and time evolutions for different values of ω are shown: (a, d) $\omega = 0.0129$; (b, e) $\omega = \omega_0 = 0.0217$; (c, f) $\omega = 0.0247$; using the parameter values $R = 5.23$, $\delta = 5.895$, $f = 0.798$, $M = 1.05$, $c = 6.798$, $d = 3.13$, $s = 0.675$, $\gamma = 0.5$.

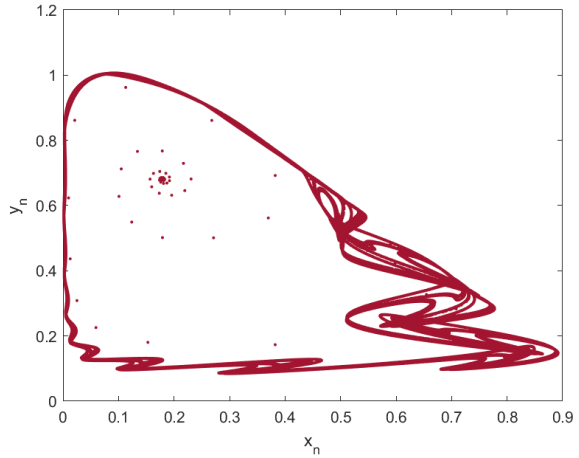

(a) Phase portrait for $\omega = 0.178$.

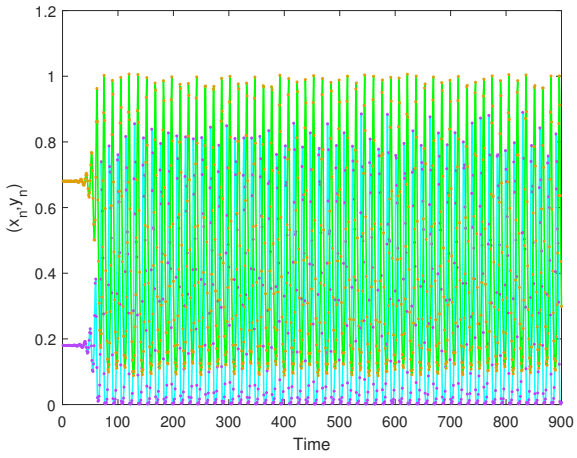

(b) Time series for $\omega = 0.178$.

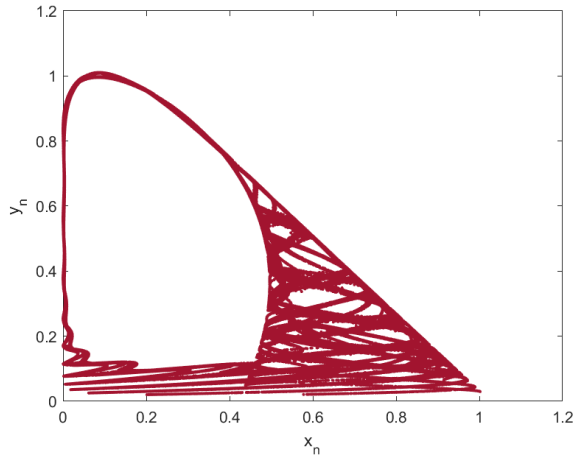

(c) Strange attractors.

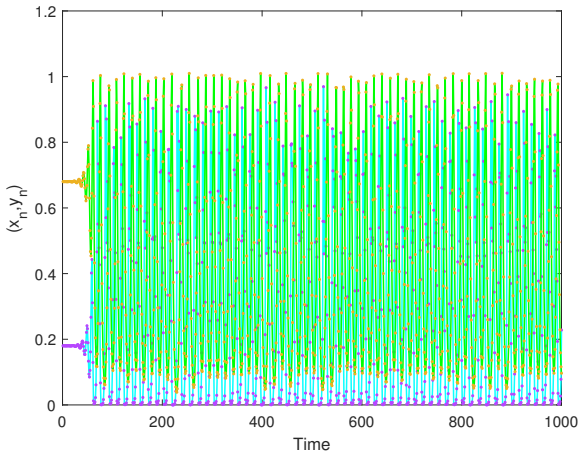

(d) Time series for $\omega = 0.1849$.

Figure 4. These graphs illustrate the strange attractors and time series of system (3.2) for the parameter values $R = 5.23$, $\delta = 5.895$, $f = 0.798$, $M = 1.05$, $c = 6.798$, $d = 3.13$, $s = 0.675$, $\gamma = 0.5$, with $\omega = 0.178$ (a, b) and $\omega = 0.1849$ (c, d).

Example 8.2. *The flip bifurcation is explained in this example under the values* $\mathrm{I}_0 = (0.71, 0.3)$*, and the parameters* $R = 2.97$*,* $\delta = 4.10$*,* $f = 01.95$*,* $M = 0.571$*,* $c = 3.89$*,* $d = 1.7$*,* $s = 0.63$*,* $\gamma = 0.5$*, and* $\omega \in [0, 0.8]$*. System* (3.2) *experiences a flip bifurcation with these parameters when the bifurcation parameter* ω *reaches* $\omega_1 = 0.4290$*. This bifurcation can be validated by constructing the Jacobian matrix at the appropriate point as*

$$\mathcal{J}_{\mathcal{P}} = \begin{pmatrix} -1.0222 & -0.8717 \\ 0.0510 & 1.0000 \end{pmatrix},$$

whose characteristic equation is

$$\mathcal{F}_{\mathcal{J}}(\kappa) = \kappa^2 + 0.0222\,\kappa - 0.9778.$$

Hence, $\kappa_1 = -1$ *and* $\kappa_2 = 0.9778$*, with* $|\kappa_2| \neq 1$*. Further, we obtain*

$$\begin{aligned}
&\Delta_0^{\mp}(q) = 1 > 0,\\
&\Delta_1^{+}(q) = 1 + \det(\mathcal{J}) = 0.0222 > 0,\\
&(-1)^2 \mathrm{F}_{\mathcal{J}}(-1) = 1 + \mathrm{Tr}(\mathcal{J}) + \det(\mathcal{J}) = -3.9968 \times 10^{-15} \approx 0,\\
&\mathrm{F}_{\mathcal{J}}(1) = 1 - \mathrm{Tr}(\mathcal{J}) + \det(\mathcal{J}) = 0.0445 > 0.
\end{aligned}$$

Note that the flip bifurcation takes place at $\omega_1 = 0.4290$*. The bifurcation diagrams of* x_n *(Figures 5(a),(b)) show that the positive fixed point* $\mathcal{P}$ *of system* (3.2) *remains stable for* $0 < \omega < 0.4290$*. Upon approaching or exceeding* 0.4290*,* ω *forces this fixed point to lose stability through a flip bifurcation. Furthermore, the system faces several instances of flip bifurcations that result in periodic orbits with lengths of* $2, 4$*, and* 8 *(see Figure 5(a)) and ultimately cause chaotic dynamics for specific values of* ω*. Figure 5(b) displays the corresponding maximal Lyapunov exponents, demonstrating that chaotic behavior and periodic orbits coexist in the parameter space. Additionally, Figure 5(b) indicates that some maximal Lyapunov exponents are negative, while others are positive, indicating the existence of periodic orbits or stable equilibria coexisting with chaos. In Figure 6, we present the phase portraits and time series for this scenario, highlighting a cascade of period-doubling bifurcations. The model displays periodic oscillations with periods* $2, 4$*, and* 8*, as illustrated in Figures 6(c)–(f). This sequence ultimately evolves into chaotic dynamics, clearly observed in Figures 6(g),(h).*

Flip bifurcations in phytoplankton-zooplankton systems signify a change from regular, stable population cycles to more complicated, alternating dynamics. From the viewpoint of ecology, this shift implies heightened susceptibility and diminished predictability, potentially resulting in significant population swings that affect the aquatic environment as a whole.

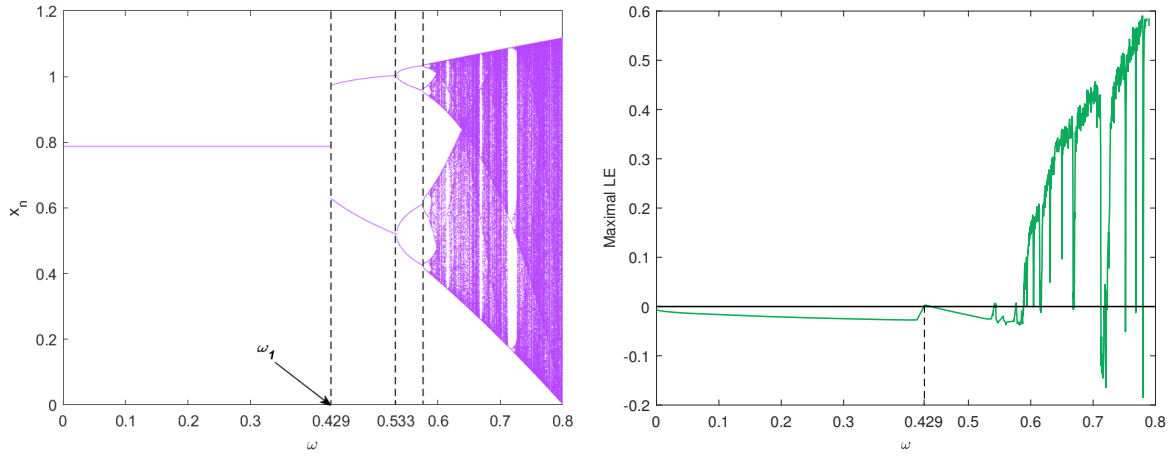

(a) Bifurcation diagram for x_n.

(b) Maximum Lyapunov exponents.

Figure 5. (a) Flip bifurcation diagram of system (3.2). (b) Corresponding maximum Lyapunov exponents for the parameter values: $R = 2.97$, $\delta = 4.10$, $f = 01.95$, $M = 0.571$, $c = 3.89$, $d = 1.7$, $s = 0.63$, $\gamma = 0.5$, and $\omega \in [0, 0.8]$.

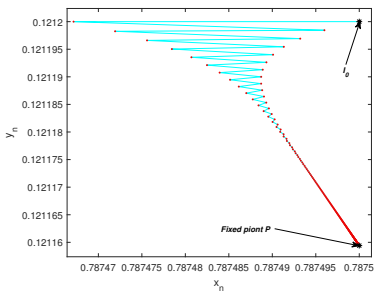

(a) Fixed point stable.

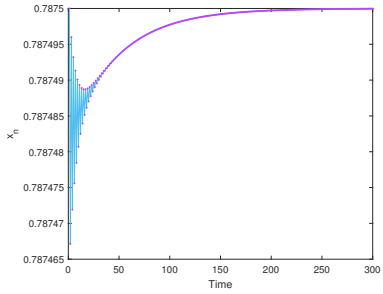

(b) Time evolution for $q = 0.45$.

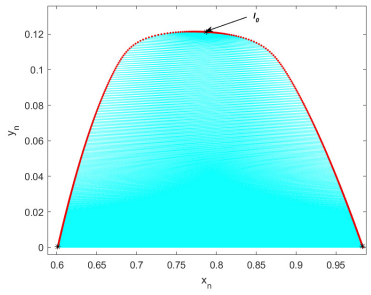

(c) 2-Period stable.

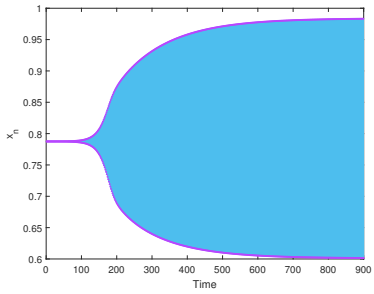

(d) Time evolution for $q = 0.45$.

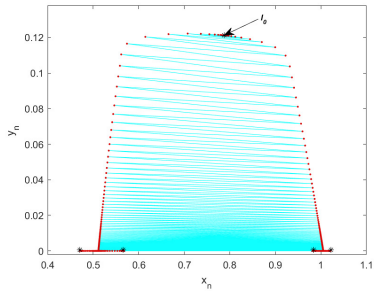

(e) 4-Period stable.

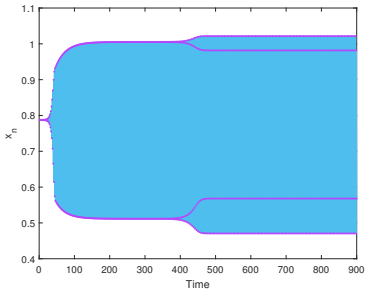

(f) Time evolution for $q = 0.543$.

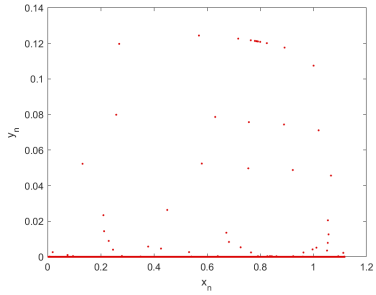

(g) Chaotic region.

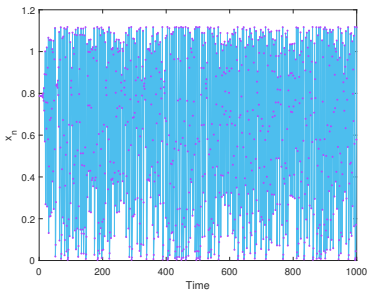

(h) Time evolution for $q = 0.8$.

Figure 6. Phase portraits and time evolutions of system (3.2) for different values of $R = 2.97$, $\delta = 4.10$, $f = 01.95$, $M = 0.571$, $c = 3.89$, $d = 1.7$, $s = 0.63$, $\gamma = 0.5$, and $\omega \in [0, 0.8]$.

9. Results and discussion

Here, we discuss the principal findings generated from the computational simulations and analytical examination of the fractional-order phytoplankton-zooplankton (PZ) model controlled by the Caputo fractional derivative. We utilized the piecewise constant argument approach to convert system (1.1) into system (3.2). The nonlinear steady-state system (3.2) was solved in order to establish the system's equilibrium points which are a trivial point and a phytoplankton-only equilibrium point. The trivial point $O = (0, 0)$ is a saddle or source as shown in Theorem 4.1 while the semi-trivial fixed point $\mathcal{E}$ becomes a sink, source, and saddle point under some conditions given in Theorem 4.2. However, if $c > d + s$ and $R(c - d - s) > sf(R + M)$, system (3.2) has a unique positive fixed point $\mathcal{P}$ as illustrated in Eq (4.1). This point is called a co-existence equilibrium point where both populations persist. The conditions under which this point is stable or unstable are given in Theorem 4.3.

System (3.2) encounters certain types of bifurcation. In particular, a subcritical Neimark-Sacker bifurcation occurs in the system for $\mathrm{L} < 0$, leading to a stable invariant closed curve that encircles $\mathcal{P}$. Moreover, a supercritical Neimark-Sacker bifurcation happens when $\mathrm{L} > 0$, producing an unstable invariant closed curve near the fixed point $\mathcal{P}$. As shown in Example 8.1 and Figures 2–4, for the parameters $R = 5.23$, $\delta = 5.895$, $f = 0.798$, $M = 1.05$, $c = 6.798$, $d = 3.13$, $s = 0.675$, $\gamma = 0.5$, and $\omega \in [0, 0.1849]$, as well as the initial conditions $I_0' = (0.12, 0.72)$, we investigate system (3.2). Using ω as the bifurcation parameter, we find that a Neimark-Sacker bifurcation occurs at $\omega_0 = 0.0217$, where the positive fixed point $\mathcal{P}$ becomes unstable. From an environmental point of view, it is the loss of stability of a fixed point and the development of long-term oscillations along a closed invariant curve, commonly in the form of quasi-periodic cycles, which may eventually result in frequency locking or chaotic dynamics. Regarding the flip bifurcation, system (3.2) experiences a flip bifurcation under the values $\mathrm{I} = (0.71, 0.3)$, and the parameters $R = 2.97$, $\delta = 4.10$, $f = 01.95$, $M = 0.571$, $c = 3.89$, $d = 1.7$, $s = 0.63$, $\gamma = 0.5$, and $\omega \in [0, 0.8]$ when the bifurcation parameter ω reaches $\omega_1 = 0.4290$. In phytoplankton-zooplankton systems, flip bifurcations indicate a transition from typical, steady population cycles to more intricate, alternating dynamics. Ecologically speaking, this change suggests increased vulnerability and less predictability, which could lead to large population fluctuations that impact the entire aquatic ecosystem.

In order to more accurately assess the advantages of the fractional formulation, we compare the integer-order model $\gamma = 1$ [19] with the fractional-order model $0 < \gamma < 1$. The fractional version showed improved stability, reduced oscillation amplitude, and delayed bifurcation. These features align with the ecological memory and delayed responses commonly seen in plankton environments. Consequently, the fractional strategy presents a more biologically accurate representation of predator-prey interactions in addition to generalizing the integer-order model.

10. Conclusions

In this work, we analyzed the equilibrium states, stability conditions, and bifurcation mechanisms of a fractional-order phytoplankton–zooplankton model which is governed by the Caputo fractional derivative. We were able to more accurately understand the qualitative dynamics of the original model by converting it into a discrete-time system utilizing the piecewise constant argument methodology. Three categories of equilibrium points were distinguished: The coexistence equilibrium $\mathcal{P}$, the

phytoplankton-only equilibrium $\mathcal{E}$, and the trivial equilibrium O. In addition, we found that the system experiences considerable nonlinear dynamics such as flip and Neimark-Sacker bifurcations. A supercritical Neimark–Sacker bifurcation produces unstable invariant curves that could cause quasi-periodic oscillations and even chaotic dynamics, whereas a subcritical bifurcation provides stable invariant closed curves around the coexistence point within particular parameter domains. The occurrence of flip bifurcations additionally represents a transition from periodic, stable solutions to complicated, alternating population cycles. In particular, based on the research results, fractional dynamics are essential for capturing long-term dependence in aquatic environments from the biological point of view. Flip bifurcations in phytoplankton-zooplankton ecosystems represent the transition from normal, stable population cycles to more complicated, alternating dynamics. From an ecological perspective, this modification indicates more susceptibility and reduces predictability, which might result in significant population oscillations. These oscillations affect the aquatic environment as a whole.

Use of Generative-AI tools declaration

The author declares he has not used Artificial Intelligence (AI) tools in the creation of this article.

Conflict of interest

The author declares that he has no conflicts of interest regarding the publication of this paper.

References

1. S. Daun, J. Rubin, Y. Vodovotz, G. Clermont, Equation-based models of dynamic biological systems, *J. Crit. Care*, **23** (2008), 585–594. https://doi.org/10.1016/j.jcrc.2008.02.003
2. V. Volpert, S. Petrovskii, Reaction-diffusion waves in biology: New trends, recent developments, *Phys. Life Rev.*, **52** (2025), 1–20. https://doi.org/10.1016/j.plrev.2024.11.007
3. M. S. Asl, M. Javidi, Novel algorithms to estimate nonlinear fdes: Applied to fractional order nutrient-phytoplankton–zooplankton system, *J. Comput. Appl. Math.*, **339** (2018), 193–207. https://doi.org/10.1016/j.cam.2017.10.030
4. D. Priyadarsini, P. Sahu, M. Routaray, D. Chalishajar, Numerical treatment for time fractional order phytoplankton-toxic phytoplankton-zooplankton system, *AIMS Math.*, **9** (2024), 3349–3368. https://doi.org/10.3934/math.2024164
5. P. Li, R. Gao, C. Xu, Y. Li, A. Akgül, D. Baleanu, Dynamics exploration for a fractional-order delayed zooplankton–phytoplankton system, *Chaos Soliton. Fract.*, **166** (2023), 112975. https://doi.org/10.1016/j.chaos.2022.112975
6. S. Pleumpreedaporn, C. Pleumpreedaporn, J. Kongson, C. Thaiprayoon, J. Alzabut, W. Sudsutad, Dynamical analysis of nutrient-phytoplankton-zooplankton model with viral disease in phytoplankton species under atangana-baleanu-caputo derivative, *Mathematics*, **10** (2022), 1578. https://doi.org/10.3390/math10091578

7. R. Shi, J. Ren, C. Wang, Stability analysis and hopf bifurcation of a fractional order mathematical model with time delay for nutrient-phytoplankton-zooplankton, *Math. Biosci. Eng.*, **17** (2020), 3836–3868. https://doi.org/10.3934/mbe.2020214
8. R. Premakumari, C. Baishya, M. E. Samei, M. K. Naik, A novel optimal control strategy for nutrient-phytoplankton-zooplankton model with viral infection in plankton, *Commun. Nonlinear Sci.*, **137** (2024), 108157. https://doi.org/10.1016/j.cnsns.2024.108157
9. C. Xu, W. Ou, Q. Cui, Y. Pang, M. Liao, J. Shen, et al., Theoretical exploration and controller design of bifurcation in a plankton population dynamical system accompanying delay, *Discrete Cont. Dyn.-S.* **18** (2024), 1182–1211. https://doi.org/10.3934/dcdss.2024036
10. I. Podlubny, *Fractional differential equations*, USA, New York: Academic Press, 1999.
11. M. Berkal, M. B. Almatrafi, Bifurcation and stability of two-dimensional activator–inhibitor model with fractional-order derivative, *Fractal Fract.*, **7** (2023), 344. https://doi.org/10.3390/fractalfract7050344
12. M. Berkal, J. F. Navarro, Qualitative behavior of a two-dimensional discrete-time prey–predator model, *Comput. Math. Methods*, **3** (2021), e1193. https://doi.org/10.1002/cmm4.1193
13. M. Berkal, J. F. Navarro, Qualitative study of a second order difference equation, *Turk. J. Math.*, **47** (2023), 516–527. https://doi.org/10.55730/1300-0098.3375
14. M. Almatrafi, M. Berkal, Bifurcation analysis and chaos control for prey-predator model with allee effect, *Int. J. Anal. Appl.*, **21** (2023), 131. https://doi.org/10.28924/2291-8639-21-2023-131
15. M. Azioune, M. S. Abdelouahab, R. Lozi, Bifurcation analysis of a cournot triopoly game with bounded rationality and chaos control via the ogy method, *Int. J. Bifurcat. Chaos*, **35** (2025), 2530019. https://doi.org/10.1142/S0218127425300198
16. M. B. Almatrafi, M. Berkal, Bifurcation analysis and chaos control for fractional predator-prey model with gompertz growth of prey population, *Mod. Phys. Lett. B*, 2550103. https://doi.org/10.1142/S0217984925501039
17. M. S. A. Elouahab, N. E. Hamri, J. Wang, Chaos control of a fractional-order financial system, *Math. Probl. Eng.*, **2010** (2010), 270646. https://doi.org/10.1155/2010/270646
18. M. Berkal, J. F. Navarro, Dynamics of a discrete-time predator-prey system with ratio-dependent functional response, *Miskolc Math. Notes*, **26** (2025), 81–99. https://doi.org/10.18514/MMN.2025.4546
19. M. S. Khan, M. Samreen, J. G. Aguilar, E. P. Careta, On the qualitative study of a discrete-time phytoplankton-zooplankton model under the effects of external toxicity in phytoplankton population, *Heliyon*, **8** (2022), e12415. https://doi.org/10.1016/j.heliyon.2022.e12415

AIMS Press